Available on: https://jnsrr.ep-journals.org/ E-ISSN: 3051-3766 P-ISSN: 3051-3758

Journal of Natural Science Research and Review

Volume: 02 Issue: 11 November-2026

Petrographic characteristics of biotite- and amphibole-bearing granites of the Sara-Fier Ring Complex, Northcentral Nigeria: insights into variations across volcanic centres

Isaac Ominyi Ajigo
Department of Applied Geology, Federal University of Technology, P.M.B. 704, Akure, Nigeria.

Published Date: November 06, 2026 **Article DOI: 10.65150/EP-jnsrr/V2E11/2026-01**

ABSTRACT: The geology of Sara-Fier igneous Complex typifies the high level, anorogenic granite suites of Northcentral Nigeria which is part of the larger Younger granite province. A combined litho-petrographical investigation using remotely-sensed as well as field and mineralogical data were carried out with a view to establishing petrographic and mineralogical variations across the complex. Progressive changes in the prevailing tectonic and petrogenetic setting at the time of emplacement of granitic rocks usually result into different petrographical and mineralogical variations of different lithologies of a rock suite. In the Sara-Fier complex, these changes manifest in visual outline of the remotely-sensed imageries where comparative clarity of display for the different rock types vary across the complex. Physiographic and petrographic changes manifest in the physical cross-sectional outlines of the volcanic centres reflecting variations in size, shape and composition of different rock types at outcrop levels as well as observable variations of minerals at the microscopic level most especially in the biotite- and hornblende-biotite granite of the complex. Mineralogical changes manifest in the shape, size, composition and mode of occurrence of the major silicate minerals as well as indicating a trend of relatively high-temperature equivalent of these minerals becoming more prevalent and persistent from north to south. This is interpreted as a progressive increase in the relative mafic affinity of the magmatic fluid from centre one up north to centre five down south; this also indicates that the original magmatic fluids are not completely identical or homogenous across the different volcanic centres.

KEYWORDS: Sara-Fier, Ring complex, Volcanic centre, Granite, Landsat.

1. INTRODUCTION

Sara and Fier, which are the type locations for the complex, are two localities within Bauchi and Plateau states respectively, cutting across Pankshin sheet 190 and Maijuju sheet 169 and lies between latitudes 9014'N and 9038'N, and longitudes 9017'E and 9030'E. Sara-Fier complex forms part of the eastern margin of the plateau Younger Granite province, standing apart from the main group of plateau Younger Granites which lies to the west and northwest, (Fig. 1). It is composed almost entirely of intrusive rocks with reportedly preserved remnants of volcanic in some places (Turner, 1971, Adubok, 2008, Aminu et al., 2017, Osinowo, et al., 2020).

The utility of remotely sensed data in geological applications such as lithological discrimination, mineral detection, mineral potential and hydrothermal alteration mapping at various scales have shown a great success (Sabins, 1999; Van der Meer *et al* 2012; Zoheir & Emam, 2014 and Kumar *et al* 2015). Spaceborne multispectral sensors, particularly Landsat Thematic Mapper (TM) and Enhanced Thematic Mapper (ETM+) launched in 1982 and 1999 with 5 and 8 spectral channels respectively have been well employed for such applications for regional mapping, structural interpretation and to aid prospection of mineral deposits (van der Meer *et al* 2012, Osinowo, et al., 2020).

The Sara-fier younger granite complex demonstrated a progressive migratory sequence of magmatic plutonism giving rise to five volcanic centres. This migratory sequence with its associated dynamism could apparently results in the variation in the petrological affinities across the different centres including mineral types, shapes and sizes as well as fractures which are structural features emplaced by tectonic deformation on rocks. Structural and lithological mapping are considered very important in several aspects of geosciences such as mineral exploration (Rowan and Lathram, 1980, Osinowo, et al., 2020, Faruk et al., 2025, Umar et al., 2026), hot spring detection, hydrogeological studies (Sabins, 1996), earthquake and landslide risk assessment and site selection for engineering construction of dam and bridges (Stefouli et al., 1996). Regional study of lithological contacts using remote sensing has made significant advances in geological research in the last few decades (Rowan and Lathram, 1980). This is more so due to the fact that the occurrence of mineral deposit in any area depends on the lithology and the tectonic history.

Most of the previous studies in the area have focused more on geochemical investigations, (Bowden, 1985; Ajigo, 2014, Ajigo, and Ashano, 2014, Aga and Haruna, 2019 and 2020, Ajigo and Ayodle, 2021). There has not been detailed lithological assessment and interpretation across the different volcanic centres partly due to inaccessibility as a result of rugged topography and thick vegetation. This study therefore integrates Landsat 8 and Shuttle Radar Thematic Mapper (SRTM) in combination with field petrology to investigate lithology as well as Petrographic characteristics of biotite- and amphibole-bearing granites and their variation across the different volcanic centres of the Sara-Fier ring complex.

License: This is an open access article under the CC BY 4.0 license: https://creativecommons.org/licenses/by/4.0/

2. REGIONAL GEOLOGICAL SETTING

2.1 Geological Setting

The Younger Granite ring complexes of Nigeria form part of a wider province of alkaline anorogenic magmatism which in turn is located within a larger Pan African Mobile Belt. The Pan African mobile belt is sandwiched between the geologically more stable and older West African Craton and Congo Craton. The Younger Granite province is characterized by numerous high-level, non-orogenic granitic ring complexes that are confined to a narrow intrusive zone, extending for about 1300km from the northern Air region of Niger Republic to the margin of the Benue valley in Nigeria (Fig. 1) and some part of Cameroun (Vincent et al., 2021 and 2022, Kamaunji et al., 2026). These complexes range in age from late Paleozoic to Tertiary with Rb/Sr whole rock dating indicating that the oldest complex of Adrar Bous in the north of Niger is Ordovician in age, with progressively younger ages southwards. The most southerly ring complex of Afu is Late Jurassic in age (Bowden, 1985). These alkaline ring complexes were emplaced in various parts of the African continent, following the Pan-African Orogeny and during one or more successive periods of Phanerozoic anorogenic magmatism, (Bowden, 1985; Vail, 1989). Aeromagnetic anomalies suggest that a series of buried NE–SW lineaments of incipient rifts controlled the disposition of the individual complexes (Ajakaiye, 1983, Eti-Mbuk et al., 2015, Osinowo et al., 2020).

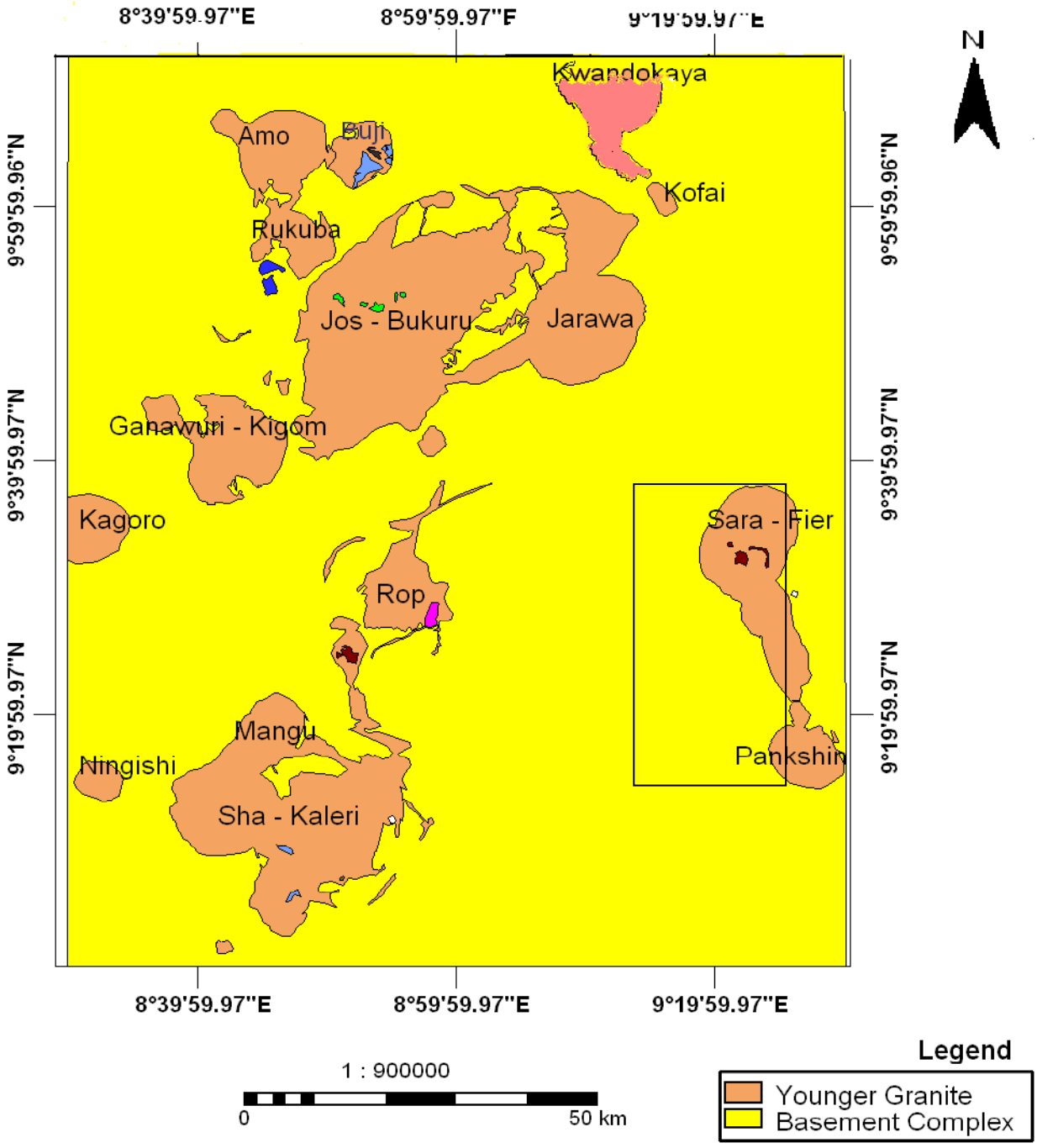


Figure 1: Sara-Fier Complex within the Younger Granite province of Jos Plateau. (Modified after Buchanam *et al.* 1971).

License: This is an open access article under the CC BY 4.0 license: https://creativecommons.org/licenses/by/4.0/

Corresponding Author: Isaac Ominyi Ajigo

2.2 Mode of Emplacement of the Younger Granite.

The evolution of the Younger Granite complexes can be summarized using a proposed model improved from the work of Ike, (1983), with five (5) main stages of emplacement. The first stage is the extrusive phase of acid volcanism which involves the build-up of a large rhyolitic volcano, forming a hood around the mouth of the vent. The volcanism was a violent paroxysmal type with upwelling of lava interspersed with explosive phases and consists of abundant pyroclastic rocks, thick intercalation of tuffs and coarse agglomerates the end of which is the sealing up of the vent (Fig.2, stage 1).

The second phase is the felsic cone-sheets and surface ring fracturing where the sealing up of the vent did not allow the eruption of the viscous phase of the acid lava; this created a gas pressure that eventually resulted in the formation of cone-sheets, occurring in swarms, and all dipping inwards to a focus. (Fig.2, stage 2). The third phase is the block subsidence and caldera phase during which the ring fractures were then filled by the highly volatile, viscous lava of quartz porphyry and the commencement of surface cauldron subsidence of the central block. The two events took place simultaneously, (Fig.2, stage 3).

The ring dyke intrusion, the fourth phase, may be regarded as an intermediate stage in the igneous cycle between the early extrusive phases of acid volcanism and the intrusive phase of emplacement of the large granite plutons. The ring dykes are of granite porphyry and their intrusion was inactive and fracture-controlled due to the low volatiles content (Fig.2, stage 4). The fifth stage is the intrusive phase of granite plutonism in which granite plutons were emplaced by the process of underground subsidence (Turner, 1989). However, the piecemeal stopping has been thought to have contributed to the upward movement of the granitic magma. In some of the ring complexes, the central vents are infilled by partially crystallized magma while in others, cone sheet-like granitic bodies are seen (fig.2, stage 5).

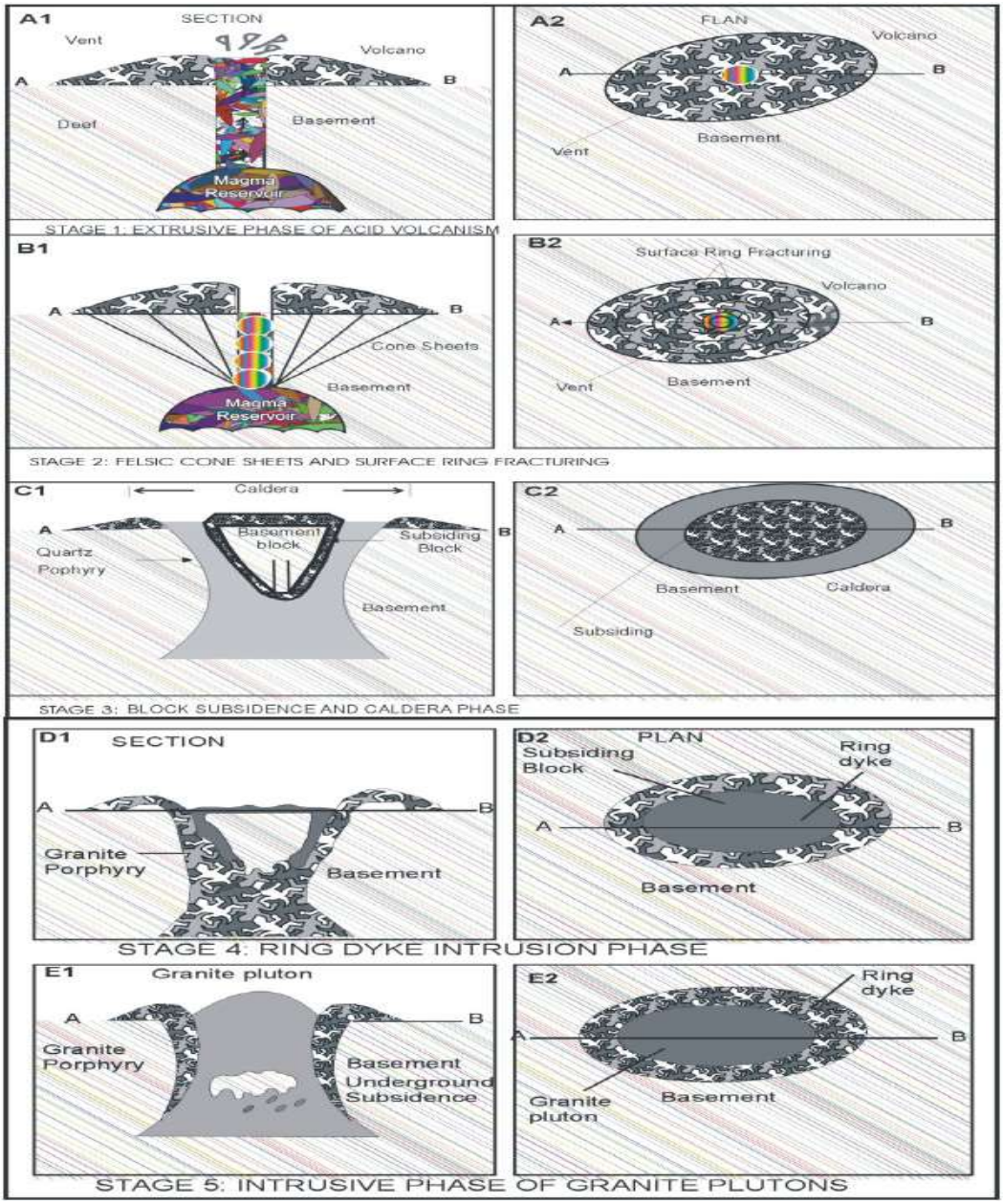


Figure 2: Model of the mode of emplacement of the Younger Granite Ring Complex. (Modified after Ike, 1983).

License: This is an open access article under the CC BY 4.0 license: https://creativecommons.org/licenses/by/4.0/

3. MATERIALS AND METHODS

The combination of satellite imageries and lithological maps were used as a guide to target volcanic centres and specific rock types of the Sara-Fier complex. Field work involved geological appraisal using base maps, satellite images and field notebook, sample collection using a geological hammer and sample bags, recording of geographic coordinates and altitudes using global positioning system (GPS) equipment as well as measurements of angular and linear features using compass and clinometers and the dimeter tape. Rocks thus targeted were studied both at outcrop as well as hand specimen level. Samples were subsequently collected for further petrographic studies. Microscopic petrography was preceded by standard thin section preparations for the purpose.

The thin sections were prepared in the laboratory and studied with the petrographic microscope. Photomicrographs were taken with digital camera and the modal content of the rocks analysed by studying the photomicrographs with *ImageJ* (Fig. 3). The procedure is as follows: Click on *File* and go to *Open* and then select the photomicrograph to be studied. The counter window will open and the selected photomicrograph will be displayed in it. Thereafter, click on *Plugins,* go to *Analyze*, select *Grid;* and then go to *Analyze* again and select *Cell Counter*. The cell counter dialogue box will be displayed. After the counting might have been completed, click on *Result* in the cell counter dialogue box to display the result in a table (Fig.2). Repeat this procedure for at least three photomicrographs taken from three different views of each thin section.

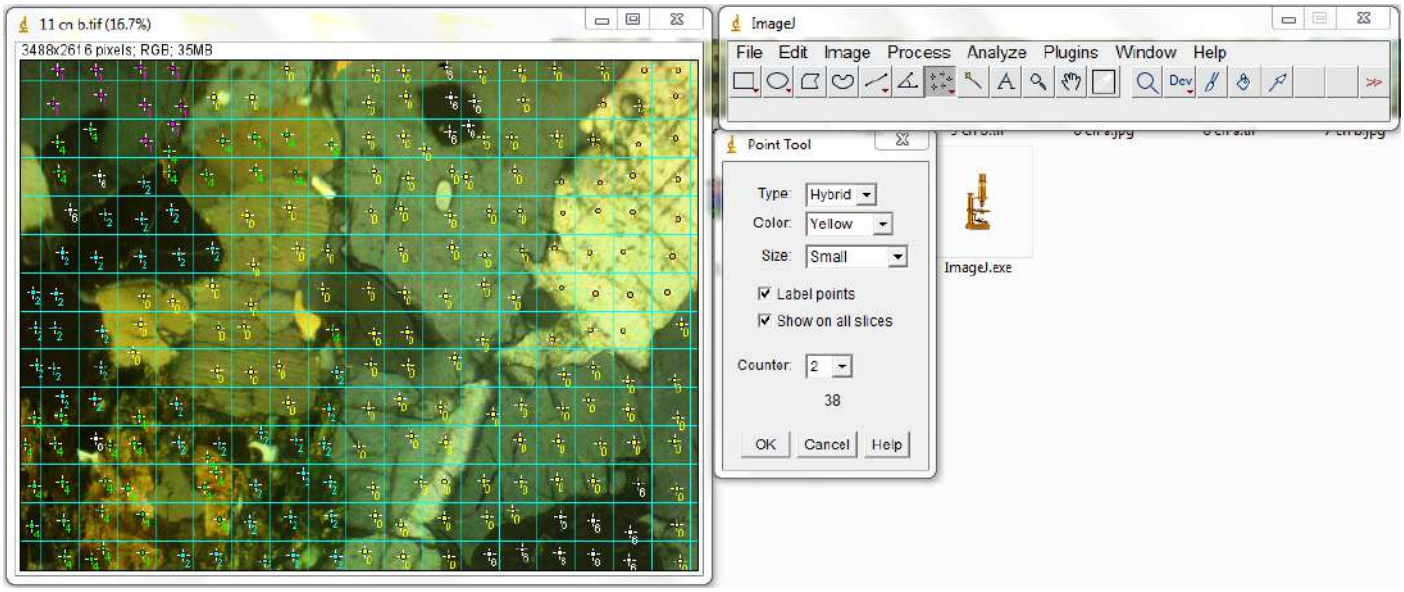


Fig. 3: Determining modal composition of rock thin sections using ImageJ.

4. RESULTS

4.1. Remote Sensing

Different layers of the processed image showed comparative clarity of display of the different granitic rock types. This necessitated the use of the different components in order to capture the different rock types in the complex. On the false colour composite map (Fig.4b), Riebeckite granite stands out with pinkish grey colour while syenite is seen to have dark grey with a bold outline. Biotite granite type I and II also stand out with high relief in the image. On the minimum noise filter (MNF) image (Fig. 4d), biotite granite type I and II, Rhyolite and hornblende-pyroxene-fayalite granite are clearly distinguishable from the image. Biotite granite type III is only partly distinguished. Biotite granite type I is most prominently outlined in the principal component analysis (PCA; Fig. 4c), followed by the hornblende-pyroxene-fayalite granite and syenite. Biotite granites type I and III are only partly distinguishable from the image. On the composite (RBG; Fig. 4a) image, Biotite granite type I and II are the most prominent while rhyolites, hornblende-pyroxene-fayalite granite and syenite are next in line. Biotite granite type III is only partly outlined.

License: This is an open access article under the CC BY 4.0 license: https://creativecommons.org/licenses/by/4.0/

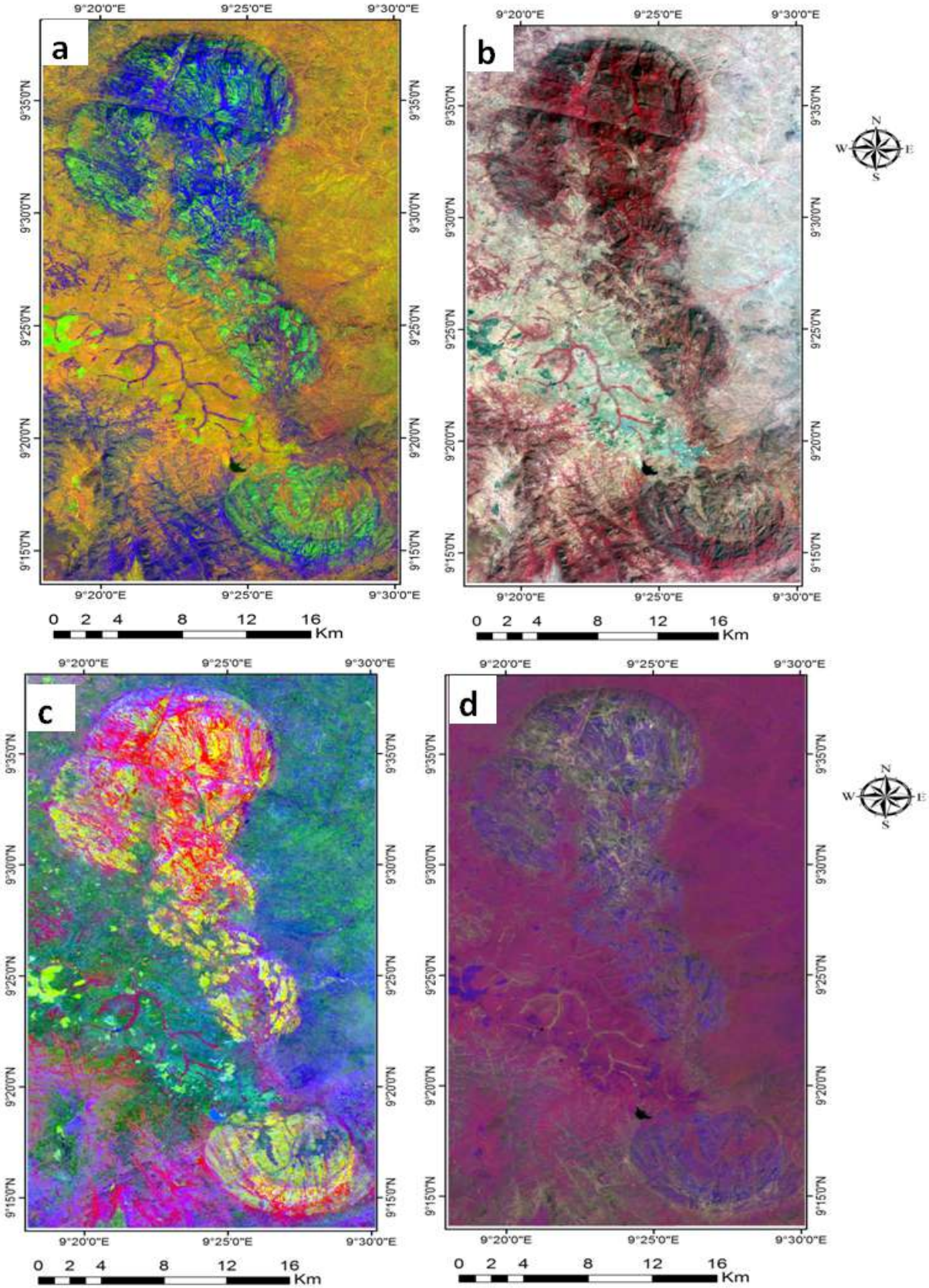


Figure 4: LandSat image of the study area displayed as: (a) Colour composite of Red, Blue and Green (b) false colour composite; (c) Principal component analysis (PCA); (d) Minimum noise fraction (MNF).

License: This is an open access article under the CC BY 4.0 license: https://creativecommons.org/licenses/by/4.0/

Corresponding Author: Isaac Ominyi Ajigo

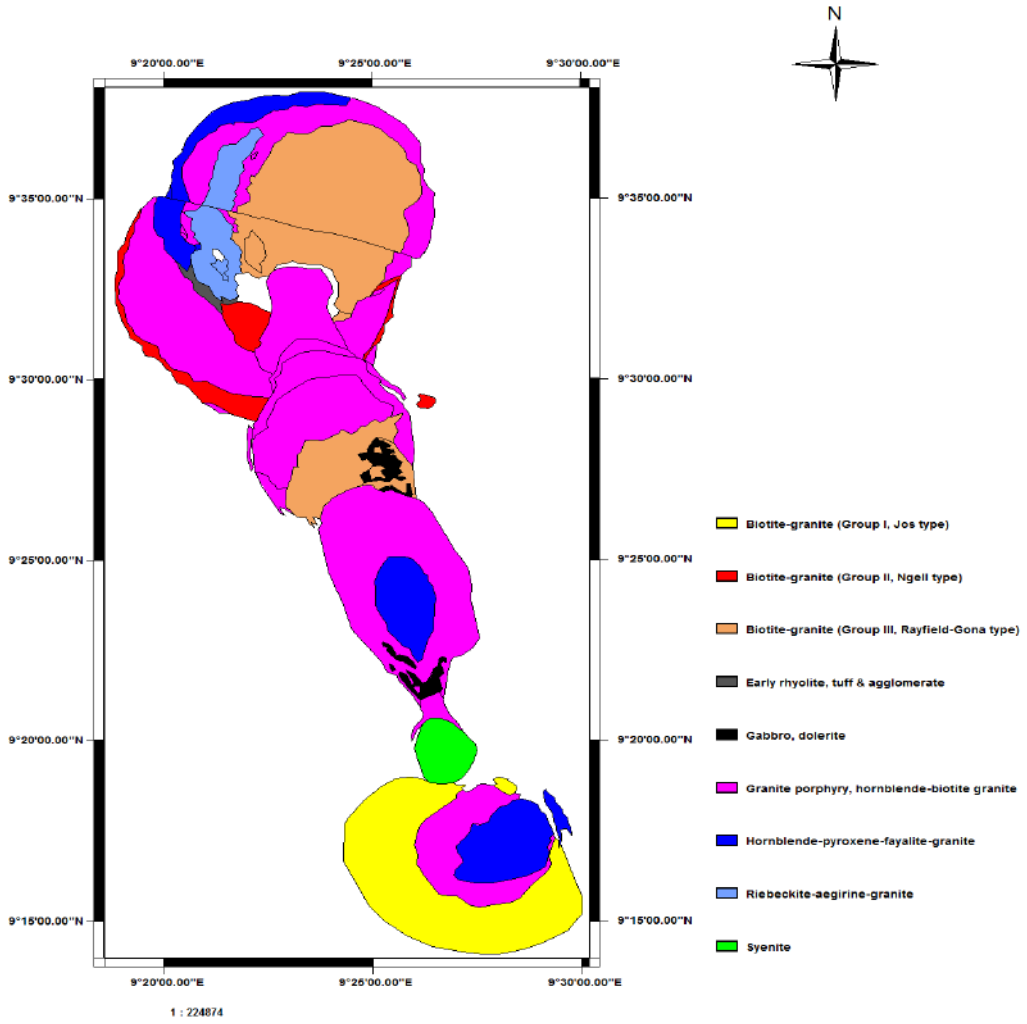


Plate 5: Geological Map of the Study Area (modified after Buchanam *et al.* 1971).

4.2. Petrographic Characteristics of Biotite Granite

4.2.1. Gonzi Biotite-Granite

The Gonzi biotite granite occupies a roughly triangular area of about 1 km^2 and situated near center one structure, forming a landscape of steep rounded hills with bare rock slabs. It intrudes into the hornblende-biotite granite and the rhyolite and basement in the southwest and north respectively. It has marginal fine-grained zone containing streak of pegmatite and occasional microgranite dykes that penetrate into surrounding rocks. It is a pink-coloured rock with variable grain size in which clusters of quartz, phenocrysts of feldspar and clots of biotite are set in a medium-grained ground mass of the same minerals.

Under the microscope, quartz forms clusters of colourless subhedral crystals evenly distributed through the slide; they are transparent and are of low relief. Feldspar is mainly cloudy perthite with irregular veins of albite-twinned plagioclase embedded in orthoclase; traces of microcline were also observed; the plagioclase feldspars are found to have alternation of white and black. Biotite shows a variety of colours: brown, yellowish-brown and reddish-brown; it occurs in irregular clusters and is pleochroic between dark and pale brown; the extinction is parallel to the cleavage traces, (Figure 6 a & b).

4.2.2. Kwappa Biotite-Granite

The kwappa biotite granite form the mountainous core of the Sara Hills, occupying over 20 km^2 in the north. Running E – W through the central part of the upland mass is the deep fault-guided Kwappa valley. It intrudes into the Sara hornblende-biotite granite and basement in the north and south respectively. Near the contacts it becomes fine-grained and develops abundant pegmatite, often as thin streaks parallel to contacts. In the southern part of the intrusion is a coarser grained pink facies in which the biotite is brown in colour. The granite is the source of alluvial cassiterite mined in and around the Kwappa valley and probably derived from thin greisens which are sometimes abundant near upper contact (Bowden, 1982, 1984, Odewumi, 2024 and 2025).

Quartz occurs in form of large, subhedral crystals, interstiticial between feldspar and biotite; some are found as intergrowth in feldspar and as inclusions in biotite; it shows colourless and transparent colour with low relief and no cleavage. Feldspar consists of free albite mainly as stumpy prisms distributed along the interfaces between large perthite and antiperthite crystals; perthite is mainly traces of microcline embedded in cloudy orthoclase. Biotite is moderately abundant, forming large flakes either as separate crystal or in clusters; it pleochroic from dark to pale brown, (Figure 6 c & d).

License: This is an open access article under the CC BY 4.0 license: https://creativecommons.org/licenses/by/4.0/

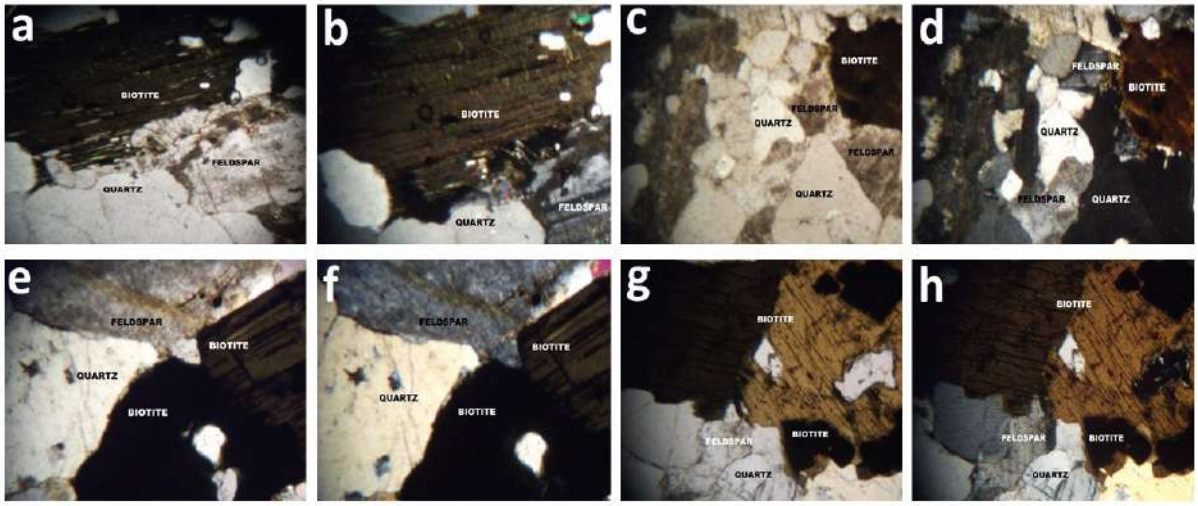


Figure 6: Photomicrograph of biotite granite: (a) [PPL] and (b) [XPL]: showing contact between biotite, quartz and feldspar; biotite showing alteration in the Gonzi biotite-granite; (c) [PPL] and (d) [XPL]: showing stumpy prisms of albite embedded in orthoclase feldspar at contact Between quartz, feldspar and biotite of Kwappa biotite-granite; (e) [PPL] and (f) [XPL]: showing Biotite in different shades of colour in contact in the Kadung biotite-granite; (g) [PPL] and (h) [XPL]: showing Biotite in various shades of colour and showing alteration in the Wulmi biotite-granite. (All magnification = *40).

4.2.3. Kadun Biotite-Granite

The Kadun biotite granite occupies the southern part of volcanic centre 3 and intrudes into the two earlier hornblende-biotite granites and also cut through the early ring dyke in the southwest. In the north and west the contacts dip gently outwards, becoming steeper in the northwest. The rock is fine-grained whitish granite with a chilled pegmatite-bearing outer margin. It is the source of alluvial cassiterite worked in the Takkos district, probably derived from the roof zone of the intrusion (Odewumi, 2024, Kamaunji et al., 2026).

Quartz occur in form of large euhedral crystals; they form interlocking grains of crystals; they also occur as inclusions within biotite; the crystals show some signs deformation by way of cracks across some of the crystals; it has a shade of colours under cross nicol between dark grey and yellow. Feldspar occurs in form of patchy microcline embedded in cloudy orthoclase; it also occur in form of large prisms and small laths of albite-twinned plagioclase; the twin lamellae are of varying width. Biotite occurs in various shades of colour, from dark brown to light brown and then green; it occurs in small plates, often surrounded by a feathery growth of green biotite; it exhibits parallel extinction. The main biotite pleochroic from dark to greenish- brown, (Figure 6 e & f).

4.2.4. Wulmi Biotite-Granite

This is an early biotite granite that has an annular outcrop around the margins of the volcanic centre 3 structure and having some of the most rugged topography of the complex. It has an irregular outline in the northwest where it develops a broad pegmatitic marginal facies. It is a coarse-grained granular rock with clusters and trails of rounded quartz grains and plates of biotite set in an aggregate of anhedral pinkish feldspar. It becomes finer grained and white in colour towards the margin and contains abundant knots of pegmatite near the outer contact.

Quartz occurs as clusters, mostly in the interstices and as inclusions within biotite; it shows low relief and has no cleavage; it shows colourless and transparent colour. Feldspar consists of perthite which forms large interlocking grains with patchy, well-twinned plagioclase being rather cloudy. Small prismatic albite are concentrated along the perthite interfaces and larger grains of albite are also grouped around clots of biotite; the plagioclase exhibits alternation of white and black bands which are not well defined. Biotite shows variety of colours from dark brown to light brown to light green; it is pleochroic between light green and dark brown and has parallel extinction, (Figure 6 g & h).

Table 1: Modal Estimate for biotite- and Hornblende-Biotite Granite of Sara-Fier complex

	Gonzi Biotite-Granite T5 (2)	Kwapa Biotite-Granite K2 (4)	Kadun Biotite-Granite T18(13)	Wulmi Biotite-Granite P10(21)	Gilling Hb-Bt-Granite T1 (1)	Gonzi Hb-Bt-Granite T8 (6)	Kumbul Hb-Bt-Granite T23(15)	Fier Hb-Bt-Granite P4 (18)
Mineral component	**Mineral percentages (%)**							
Quartz	29	27	27	30	25	26	24	25
Feldspar	57	59	59	57	49	51	55	56
Biotite	11	11	12	12	12	10	10	11
Amphibole	-	-	-	-	10	9	8	9

License: This is an open access article under the CC BY 4.0 license: https://creativecommons.org/licenses/by/4.0/

Corresponding Author: Isaac Ominyi Ajigo

Pyroxene	-	-	-	-	1	-	-	-
Accessories	2	3	2	1	2	3	1	2
Total	**99**	**100**	**100**	**99**	**99**	**99**	**100**	**100**

4.3. Petrographic Characteristics of Hornblende-Biotite Granite

4.3.1. Gilling Hornblende-Biotite-Granite of volcanic Centre 1

This occupies roughly 14 km^2 in the southern Sara hills where it forms a broad crescent separated into two parts by the latter intrusion. It is a coarse-grained grey rock with quartz grains of about 5mm in diameter forming trails set in a mass of larger interlocking feldspar. The north-eastern margin of the main outcrop is largely a mechanical junction with the rhyolites and the original extent giving an indication that it was considerably greater than the present outcrop, perhaps occupying the whole of volcanic centre 1.

Quartz occurs as subhedral crystals forming trails set in a mass of larger interlocking feldspars; it is colourless and transparent; it has low relief and no cleavage. Feldspar occurs both as perthite and separate albite-twinned plagioclase; the plagioclase are found embedded within the orthoclase feldspars (Figure 7 a & b); the twin lamellae of the plagioclase are not perfect as they are not well-defined; orthoclase appear cloudy only in places and is being replaced by biotite in places. Biotite occurs as net-like isolated crystals as well as replacement of feldspar in places; it pleochroic between brown and yellowish brown; it is brown in colour and is of moderate relief. Amphibole occurs as clusters of subhedral crystals of dark-green hornblende, standing out with high relief and with cleavage planes in two direction at angles of about 59^0 and 121^0; it pleochroic between green and brown.

4.3.2. Gonzi Hornblende-Biotite-Granite

The Gonzi hornblende-biotite-granite is a compact, stock-like body of about 5 km2 in extent, situated just to the east of Gonzi and lying partly outside the centre 2 ring structure. It juts into the centre 2 ring structure in the north and flanked by basement rocks. It shares a steep, well-exposed contact with its counterpart in centre 1 and is truncated by the later centre 3 ring structure. It is a medium-grained pinkish rock with euhedral phenocrysts of feldspar about 5mm long set in an only slightly finer-grained groundmass. It show very little marginal modification with only a foot or two of chilled rock against the contact. A characteristic of this rock is that it contains occasional small basic clots about 1cm in diameter which seem to have been derived from xenoliths of porphyritic basalt. In the normal rock, hornblende is rather rare and may be partly replaced along cleavage traces by biotite. The biotite occur mainly as separate flakes, pleochroic from green to pale yellowish brown and often partly altered to brownish chlorite.

Here, quartz occurs as large, isolated subhedral crystals, as well as in the interstices of other minerals; it is colourless and transparent with those in the interstices appearing cloudy; it of low relief. Feldspar consists of a few euhedral crystals of albite-twinned plagioclase with characteristic twinning and more abundant large crystals of orthoclase; some of the twinned plagioclase are found embedded within the larger crystals of orthoclase. Biotite occurs mainly as separate flakes of poorly formed crystals; it pleochroic between greenish-brown and yellowish-brown; it has moderate relief and is dark-brown in colour. Hornblende is rather rare and show evidence of replacement along cleavage traces by biotite; it stands out with high relief but the cleavage planes are not perfectly defined. It is dark-green in colour and pleochroic between green and brown, (Figure 7 c & d).

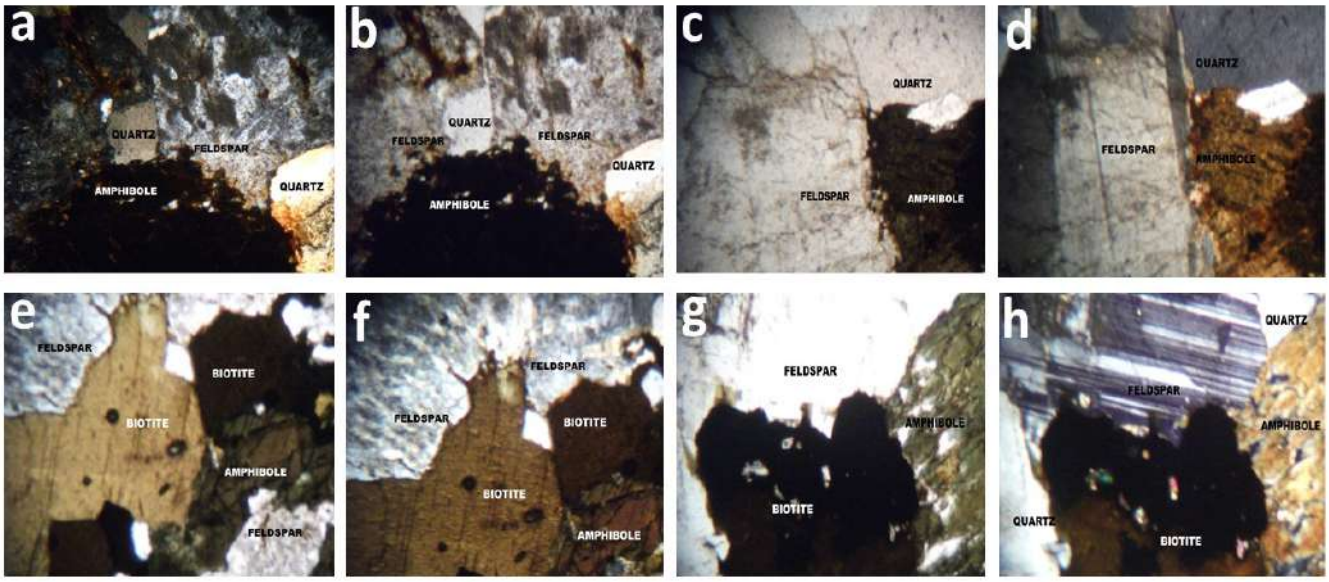


Fig.7 (a) [PPL] and (b) [XPL]: showing imperfect plagioclase embedded within orthoclase feldspar of the Gilling hornblende-biotite-granite; (c) [PPL] and (d) [XPL]: showing contact between feldspar, quartz and amphibole of the Gonzi hornblende-biotite-granite; (e) [PPL] and (f) [XPL]: showing contact between feldspar, quartz, biotite and amphibole in the Kumbul hornblende-biotite-granite; (g) [PPL] and (h) [XPL]: showing Quartz occurring as interstitial pool within biotite, amphibole and Feldspar in the Fier hornblende-biotite-granite. (All magnification = *40).

License: This is an open access article under the CC BY 4.0 license: https://creativecommons.org/licenses/by/4.0/

4.3.3. Kumbul Hornblende-Biotite-Granite

The Kumbul hornblende-biotite-granite outcrops as broad crescent enclosed within the northern part of the outer ring-dyke. It intrudes its Takkos counterpart in the northern and western contact and it is of identical grain size with the latter with gradational contacts in places. It is medium-grained and porphyritic with phenocrysts of pinkish feldspar set in an area in which phenocrysts are sparse and the groundmass finer in grain.

Quartz forms the interstices between other minerals; it is made up of small subhedral crystals of low relief; it is colourless and transparent in colour and also occurs as cloudy, transparent patches within the feldspar. Feldspar is mostly perthite with large crystals of orthoclase within which traces of microcline are embedded; the microcline exhibits characteristic cross-hatched twinning; the orthoclase show well-defined outlines at the boundaries with other minerals. Amphibole is present in form of hornblende which forms separate subhedral crystals or irregular clustered grains; they show well-defined cleavage planes in two directions and with angles of about 58^0 and 222^0; zoning is also observed in a few crystals; it is green in colour and pleochroic between light green and greenish brown, (Figure 7 e & f). Biotite is either associated with the hornblende or in large separate plates; the isolated ones appear surrounding the hornblende crystals while the associated ones are found within the amphiboles; it of moderate relief and brown in colour.

4.3.4. Fier Hornblende-Biotite-Granite

The Fier hornblende-biotite granite occupies the broad outer rim of the Fier hills with an annular with of more than 1km. The outer contacts are against basement. The north-western contact is against the Kadun biotite granite of centre 3. It is a fairly coarse-grained granular rock. Where the granite comes against the basic rocks to the north and south, it is contaminated, becoming finer-grained and porphyritic and containing fine-grained clots consisting of biotite, quartz and plagioclase, with a little hornblende and numerous tiny apatite needles.

Quartz forms clusters of anhedral grains, set between large interlocking crystals of perthite; they show random distribution with low relief and no cleavage. Feldspar occurs as mostly perthite with occasional separate crystals of albite-twinned plagioclase; perthite is mostly orthoclase which form large subhedral crystals which appear in isolation as well as in the interstices between crystals of amphiboles; plagioclase consist of well-formed twin lamellae; they exhibit low relief. Biotite occurs in form of isolated subhedral crystals that are found wedged between crystals of feldspar and amphiboles; they are of moderate relief and show parallel extinction. Amphibole is present in form of green hornblende occurring in subhedral crystal grains associated with biotite; it pleochroic between deep green and greenish-brown and has high relief; it shows well-defined cleavage planes in two directions at angles of about 60^0 and 120^0, (Figure 7 g & h).

5. DISCUSSION

A peculiar attribute of the younger granite complex is the fact that not all rock types are reported to be associated with mineralization as for instance, biotite-granite is mineralized in certain and not in all places. The same is applicable to the hornblende-biotite-granite. This could be attributable to progressive changes in the prevailing tectonic and petrogenetic setting at the time of emplacement. These changes is first manifest in the remotely-sensed imageries where comparative clarity of display for the different rock types vary across the Sara-Fier complex.

In addition to variations in size and shape of different rock types at outcrop levels, there is also observable variations of minerals at the microscopic level. While quartz forms clusters of colourless subhedral crystals that are evenly distributed across the Gonzi biotite-granite, it is largely interstitial between feldspar and biotite in the Kwappa biotite-granite. It however occurs partly as inclusions within biotite in the Kadun and Wulmi biotite-granite. Feldspar in the Gonzi biotite-granite occur mainly as cloudy perthite with irregular veins of albit-twinned plagioclase embedded in orthoclase and with traces of microcline while in the Kwappa biotite granite, it consists of free albite mainly as stumpy prisms distributed along the interfaces between large perthite and antiperthite crystals and perthite consisting mainly of traces of microcline embedded in cloudy orthoclase. In the Kadun biotite granite, Feldspar occurs in form of patchy microcline embedded in cloudy orthoclase; it also occur in form of large prisms and small laths of albite-twinned plagioclase; the twin lamellae are of varying width while in the Wulmi biotite granite it consists of perthite which forms large interlocking grains with patchy, well-twinned plagioclase being rather cloudy; also in the Wulmi biotite granite, small prismatic albite are concentrated along the perthite interfaces and larger grains of albite are also grouped around clots of biotite.

In the Gonzi biotite-granite, biotite shows a variety of colours including brown, yellowish-brown and reddish-brown, occurring in irregular clusters and is pleochroic between dark and pale brown; the extinction is parallel to the cleavage traces while in the Kwappa biotite granite, it is of moderate abundance, forming large flakes either as separate crystal or in clusters and pleochroic from dark to pale brown. In the Kadun biotite-granite, biotite occurs in various shades of colour, from dark brown to light brown and then green; it also occurs in small plates, often surrounded by a feathery growth of green biotite, exhibiting parallel extinction.

There is also observable trend of variation in shape and size of major silicate minerals of the hornblende-biotite-granite. In the Gilling hornblende-biotite-granite, Quartz occurs as subhedral crystals forming trails set in a mass of larger interlocking feldspars while in the Gonzi hornblende-biotite-granite, quartz occurs as large, isolated subhedral crystals, as well as in the interstices of other minerals; in the Kumbul hornblende-biotite-granite quartz is made up of small colourless and transparent subhedral crystals of low relief forming the interstices between other minerals and also occurs as cloudy, transparent patches within the feldspar while in the Fier hornblende-biotite-granite it forms clusters of anhedral grains, set between large interlocking crystals of perthite.

In the Gilling hornblende-biotite-granite, feldspar occurs both as perthite and separate albite-twinned plagioclase; the latter which are found embedded within the orthoclase feldspars, which themselves consist of poorly defined, imperfect and cloudy orthoclase and is being replaced by biotite in places while in the Gonzi hornblende-biotite-granite feldspar consist of more euhedral crystals of albite-twinned plagioclase and more abundant large crystals of orthoclase. In the Kumbul hornblende-biotite-granite, feldspar is mostly perthite with large crystals of orthoclase within which traces of microcline are embedded while in the Fier hornblende-biotite-granite feldspar occurs also as mostly perthite but with occasional separate crystals of albite-twinned plagioclase and perthite mostly orthoclase which form large subhedral crystals which appear in isolation as well as in the interstices between crystals of amphiboles.

License: This is an open access article under the CC BY 4.0 license: https://creativecommons.org/licenses/by/4.0/

Corresponding Author: Isaac Ominyi Ajigo

Biotite in the Gilling hornblende-biotite-granite occurs as net-like isolated crystals as well as replacement of feldspar in places while in the Gonzi hornblende-biotite-granite, it occurs mainly as separate flakes of poorly formed crystals. In the Kumbul hornblende-biotite-granite, biotite is either associated with the hornblende or in large separate plates; the isolated ones appear surrounding the hornblende crystals while the associated ones are found within the amphiboles while in the Fier hornblende-biotite granite it occurs in form of isolated subhedral crystals that are found wedged between crystals of feldspar and amphiboles.

Amphiboles of the Sara-Fier complex occur largely as hornblende and of variable abundance across the different volcanic centres for instance, in the Gilling hornblende-biotite-granite, it occurs as clusters of subhedral crystals of dark-green hornblende, standing out with high relief while in the Gonzi hornblende-biotite-granite, hornblende is rather rare and show evidence of replacement along cleavage traces by biotite. In the Kumbul hornblende-biotite-granite, hornblende forms separate subhedral crystals or irregular clustered grains showing well-defined cleavage planes and zoning observed in a few crystals while in the Fier hornblende-biotite granite, amphibole is present in form of green hornblende occurring in subhedral crystal grains associated with biotite.

Physical properties of minerals such as crystallinity (either euhedral, subhedral or anhedral as well as shape, size and position of formation (either as perthite, antiperthite, interstitial or interlocking) are a direct reflection of the prevailing conditions during emplacement of magmatic rocks. In the Sara-Fier complex, these changes are manifested across the different volcanic centres as represented by the different major silicate minerals such as quartz, feldspar, biotite and amphibole. A petrogenetic significance of this suit of rocks is the fact that relatively high-temperature equivalent or varieties of minerals such as biotite, feldspar, and amphiboles are more prevalent and persistent as one moves from centre one up north down to centre five. This indicates that there is a progressive increase in the relative mafic affinity of the magmatic fluid from centre one up north to centre five down south. This equally indicates that the original magmatic fluids are not completely identical or homogenous across the different volcanic centres.

The physical cross-sectional outlines of the volcanic centres also indicate that centre one and two are more symmetrical, almost superimposed on one another whereas centres three, four and five are elongated in outline. Volcanic centre two tend to be the most extensive having eaten up parts of centre one and probably enhanced by the latter and both consequently having the most rugged topography (Figure 8).

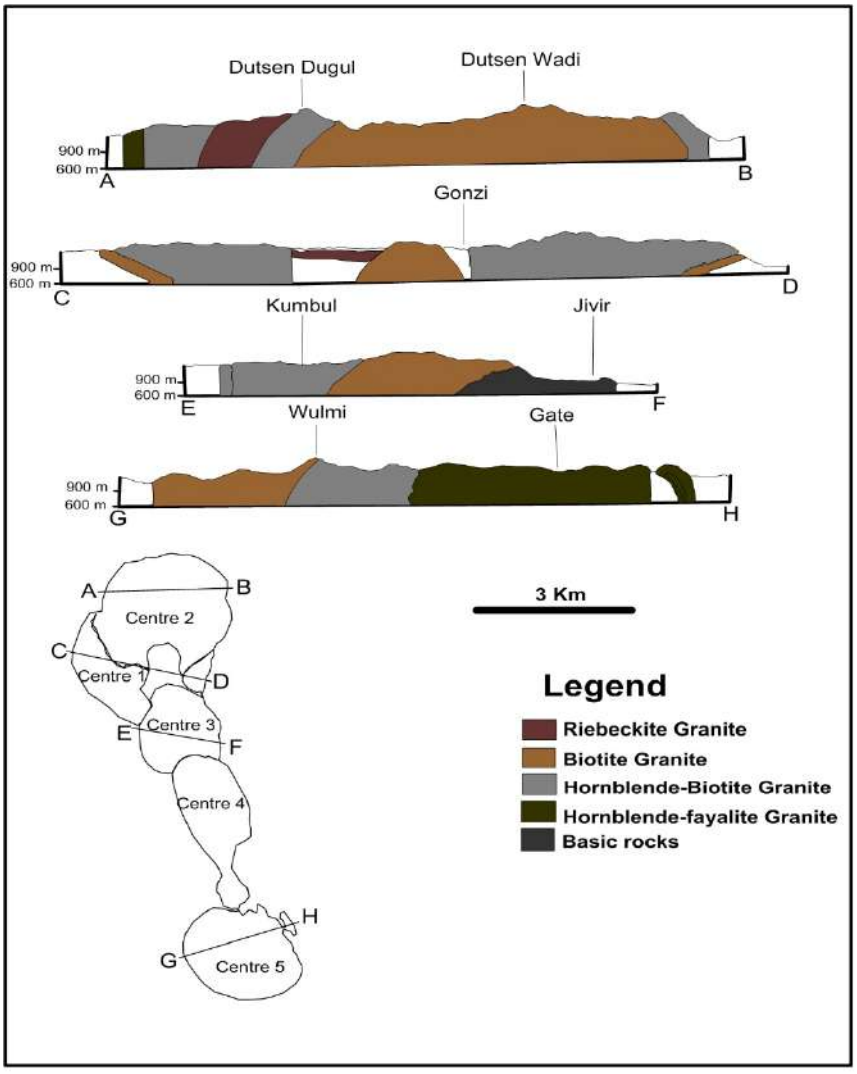


Figure 8: Geological cross section across the Sara-Fier Complex (Modified after Buchanam et al., 1971)

License: This is an open access article under the CC BY 4.0 license: https://creativecommons.org/licenses/by/4.0/

6. CONCLUSION

The remote sensing approaches in lithological discrimination are influenced by difference in response of different rock types to the different portions of the electromagnetic spectrum. It is therefore possible to generate a predictive surficial geology map, based on remote sensing data, which broadly defines the main surficial geology of an area. While the remote-sensing-derived map is no substitute for good field mapping, it has the most value in areas where the surficial geology is either very poorly known or not easily accessible. Where poorly known, it provides a preliminary reconnaissance tool.

The fact that not all rock types within the Younger granite province are reported to be associated with mineralization is a peculiar attribute of these rock where certain rocks at certain locations are mineralized while their counterparts in other locations are not. This could apparently be attributable to progressive changes in the prevailing tectonic and petrogenetic setting at the time of emplacement. These changes not only manifest in the remotely-sensed imageries where comparative clarity of display for the different rock types vary across the complex due to their inherent dissimilarities, but also reflect in variations in size, shape and composition of different rock types at outcrop levels as well as observable variations of minerals at the microscopic level most especially in the biotite- and hornblende-biotite granite of the Sara-Fier Younger granite complex.

REFERENCES

1) Adubok, A. S. (2008). Evolutionary trend of the Jarawa Younger Granites Ring Complex, Jos Plateau, Central Nigeria. *Science World Journal, 3*(2), 1 - 15
2) Aga, T., & Haruna, A. I. (2020). The petrogenesis and tectonic setting of Sara-Fier Younger Granite Complex, Central Nigeria. *Journal of Scientific Research, 64*(1), 8–19.
3) Aga, T., & Haruna, A. I. (2019). The field and petrographic studies of the Sara-Fier Granite Suite, Central Nigeria. *OnLine Journal of Earth Sciences, 13*(1), 1–9.
4) Ajakaiye, D.E. (1983): Deep structures of alkaline ring complexes from geophysical data. In: Abstract, international conference on alkaline ring complexes in Africa. Zaria, Nigeria
5) Ajigo, I. O., & Ayodele, O. S. (2021). Litho-structural analysis of the Sara-Fier Ring Complex, Northcentral Nigeria. *International Journal of Earth Science and Geophysics, 7*, 055, 1 - 11
6) Ajigo, I.O. and Ashano, E.C. (2014): Biotite composition and magma type (petrogenesis) of Sara-Fier Complex, Northcentral Nigeria. *Journal of Mining and Geology, 50(2) 99-108.*
7) Ajigo, I.O. (2014): Geochemical Characteristics of Amphiboles from Sara-Fier Complex, North Central Nigeria. International Journal of Advances in Earth Sciences, Volume 3, Issue 1, 24-31.
8) Aminu, M. D., Ardo, B. U., & Jato, M. A. (2017). A bibliography of geological studies on the Younger Granites Ring Complexes of Nigeria: 1951–2015. *Oil & Gas Research, 3*,
9) Bowden P (1982): Magmatic evolution and mineralisation in the Nigerian Younger Granite province. In: Evans AM (ed) Metallisation associated with acid magmatism. John Wiley, London
10) Bowden P, Kinnaird JA (1984): Geology and mineralization of the Nigerian anorogenic ring complexes. Geologisches Jahrb (Hannover) B56, 3–65
11) Bowden P (1985): The geochemistry and mineralization of alkaline ring complexes in Africa. J Afr Earth Sci 3:17–39
12) Buchanam, M.S., MacLeod, W.N. and Turner, D.C. (1971): The Geology of the Jos Plateau. Geological Survey of Nigeria, Bulletin No. 32.
13) Eti-Mbuk, S., Akanbi, E. S., & Fakoya, A. D. (2015). Regional magnetic field trend and depth to magnetic source determination from aeromagnetic data of Maijuju area, North Central Nigeria. *Physical Science International Journal, 8*(3), 1–13.
14) Faruk, M. U., Yusuf, S. N., & Daspan, R. I. **(2025).** Integrated aeromagnetic and airborne radiometric analysis for structural mapping and mineralisation potential in the Naraguta Area, North-Central Nigeria. *Results in Earth Sciences, 3*, 100077.
15) Ike E.C. (1983). The structural evolution of Tibchi Ring complex, a case study for the Nigerian Younger Granite Province. Journal of Geological Society London, 140, 782-800.
16) Kamaunji, V. D., Ahmed, H. A., Wang, L.-X., Sanislav, I. V., Girei, M. B., Zhu, Y.-X., Liang, X.-X., Chen, X., & Sami, M. (2026). Progressive mantle melting and crust–mantle–fluid hybridization in fluorite-bearing Sn–Nb ± Mo-rich alkaline granites of the Jos Plateau, central Nigeria. *Ore Geology Reviews, 195*, 107405.
17) Kumar, C., Shetty, A., Raval, S., Sharma, R. and Ray, P.K.C. (2015): Lithological Discrimination and Mapping using ASTER SWIR Data in the Udaipur area of Rajasthan, India. *Procedia Earth and Planetary Science 11 180 – 188*
18) Odewumi, S. C. (2025). Mineralogy and heavy minerals recovery of stream sediments on the Jos Plateau, northcentral Nigeria: Implications for mineralization. *Discover Geoscience, 3*, 20. https://doi.org/10.1007/s44288-025-00124-7.
19) Odewumi, S. C. (2024). Mineralization, geochemical signatures, and provenance of stream sediments on the Jos Plateau, Northcentral Nigeria. *Journal of the Nigerian Society of Physical Sciences, 6*(4), 2181. https://doi.org/10.46481/jnsps.2024.2181.
20) Osinowo, O. O., Alumona, K., & Olayinka, A. I. (2020). Analyses of high resolution aeromagnetic data for structural and porphyry mineral deposit mapping of the Nigerian Younger Granite Ring Complexes, North-Central Nigeria. *Journal of African Earth Sciences, 162*, 103705. https://doi.org/10.1016/j.jafrearsci.2019.103705.
21) Rowan, L.C., Lathram, E.H. (1980): Mineral exploration (Chapter 17). Siegal, B.S., Gillespie, A.R. (Eds.), Remote Sensing in Geology. John Wiley and sons, New York, pp. 553–605.
22) Sabins, F. F. (1999): Remote sensing for mineral exploration. *Ore Geology Reviews*; 14(3): 157-183.
23) Sabins, F.F. (1996): Remote Sensing: Principles and Interpretation, third ed. W. H. Freeman and Company, New York, 494.

License: This is an open access article under the CC BY 4.0 license: https://creativecommons.org/licenses/by/4.0/

Corresponding Author: Isaac Ominyi Ajigo

24) Stefouli, M., Angellopoulos, A., Perantonis, S., Vassilas, N., Ambazis, N., Charou, E. (1996): Integrated Analysis and Use of Remotely Sensed Data for the Seismic Risk Assessment of the Southwest Peloponessus Greece. First Congress of the Balkan Geophysical Society, Athens Greece.
25) Turner, D. C. (1971): The Sara-Fier Complex. In: Buchanan, M.S., MacLeod, W.N. and Turner, D.C. (1971): The Geology of the Jos Plateau. Geological Survey of Nigeria, Bulletin No. 32.
26) Umar, M., Ahmed, A. L., Osumeje, J. O., & Magaji, S. S. (2026). Qualitative delineation of airborne magnetic and radiometric structures associated with cassiterite-columbite mineralization of Barikin Ladi Tin field, Jos North-Central Nigeria. *Discover Geoscience, 4*, 39. https://doi.org/10.1007/s44288-026-00408-6.
27) Van der Meer, F. D., Van der Werff, H. M., van Ruitenbeek, F. J., Hecker, C. A., Bakker, W. H., Noomen, M. F., & Woldai, T. (2012): Multi-and hyperspectral geologic remote sensing: A review. *International Journal of Applied Earth Observation and Geoinformation* 14(1): 112-128.
28) Vail, J.R. (1989). Ring complexes and related rocks in Africa. Journal of African Earth sciences. 8, 19-40.
29) Vincent, V. I., Wang, L.-X., Zhu, Y.-X., Kamaunji, V. D., Ahmed, H. A., Ntekim, E. E., & Cao, L. (2022). Onset of the anorogenic alkaline magmatism in the Nigerian Younger Granite province: Constraints from the Daura and Dutse complexes. *Lithos, 410–411*, 106561. https://doi.org/10.1016/j.lithos.2021.106561.
30) Vincent, V. I., Li, H., Girei, M. B., Ahmed, H. A., & Ntekim, E. E. (2021). Genesis and age of Pb–Zn mineralization from the Ningi-Burra Ring Complex, North Central Nigeria: Constraints from zircon morphology, U–Pb dating and Lu–Hf isotopes. *Lithos,* 106115. *390–391*,
31) Zoheir, B., & Emam, A. (2014): Field and ASTER imagery data for the setting of gold mineralization in Western Allaqi–Heiani belt, Egypt: A case study from the Haimur deposit. Journal of African Earth Sciences; 99: 150-164.

License: This is an open access article under the CC BY 4.0 license: https://creativecommons.org/licenses/by/4.0/

Corresponding Author: Isaac Ominyi Ajigo